Amino Acids (2011) 40:829–839
DOI 10.1007/s00726-010-0700-6

ORIGINAL ARTICLE

Inhibition of a bacterial *O*-GlcNAcase homologue by lactone and lactam derivatives: structural, kinetic and thermodynamic analyses

Yuan He · Abigail K. Bubb · Keith A. Stubbs · Tracey M. Gloster · Gideon J. Davies

Received: 16 April 2010 / Accepted: 13 July 2010 / Published online: 6 August 2010

Abstract The dynamic, intracellular, *O*-GlcNAc modification is of continuing interest and one whose study through targeted "chemical genetics" approaches is set to increase. Of particular importance is the inhibition of the *O*-GlcNAc hydrolase, *O*-GlcNAcase (OGA), since this provides a route to elevate cellular *O*-GlcNAc levels, and subsequent phenotypic evaluation. Such a small molecule approach complements other methods and potentially avoids changes in protein–protein interactions that manifest themselves in molecular biological approaches to *O*-GlcNAc transferase knockout or over-expression. Here we describe the kinetic, thermodynamic and three-dimensional structural analysis of a bacterial OGA analogue from *Bacteroides thetaiotaomicron*, *Bt*GH84, in complex with a lactone oxime (LOGNAc) and a lactam form of *N*-acetylglucosamine and compare their binding signatures with that of the more potent inhibitor *O*-(2-acetamido-2-deoxy-D-glucopyranosylidene)amino *N*-phenyl carbamate (PUGNAc). We show that both LOGNAc and the *N*-acetyl gluconolactam are significantly poorer inhibitors than PUGNAc, which may reflect poorer mimicry of transition state geometry and steric clashes with the enzyme upon binding; drawbacks that the phenyl carbamate adornment of PUGNAc helps mitigate. Implications for the design of future generations of inhibitors are discussed.

Keywords Carbohydrate · Enzyme · X-ray structure · *O*-GlcNAc · Diabetes · Neurodegeneration

Y. He · A. K. Bubb · T. M. Gloster · G. J. Davies (✉)
York Structural Biology Laboratory, Department of Chemistry, The University of York, York YO10 5DD, UK
e-mail: davies@ysbl.york.ac.uk

T. M. Gloster
e-mail: gloster@ysbl.york.ac.uk

Present Address:
T. M. Gloster (✉)
Department of Chemistry, Simon Fraser University, 8888 University Drive, Burnaby, BC V5A 1S6, Canada

Present Address:
K. A. Stubbs
School of Biomedical, Biomolecular and Chemical Sciences, The University of Western Australia (M310), 35 Stirling Highway, Crawley, WA 6009, Australia

Introduction

The "*O*-GlcNAc" modification, first reported by Torres and Hart (1984), is the dynamic post-translational modification of intracellular targets through the reversible incorporation of β-linked *N*-acetyl-D-glucosamine to serine and threonine residues. Since its discovery, over 600 eukaryotic proteins have been found to be *O*-GlcNAc modified (reviewed in, for example, Wells et al. 2001; Hart et al. 2007; Butkinaree et al. 2010) and this number will only increase as more experiments are performed and methods of detection improve. In mammals (this paper will not cover the roles of *O*-GlcNAc in plants, for which the reader is directed to Olszewski et al. 2010), much of the implied importance of *O*-GlcNAc reflects its cross talk and potential reciprocity with phosphorylation (recently reviewed in Butkinaree et al. 2010). The interplay with phosphorylation, together with the cellular targets for the *O*-GlcNAc modification, implicates *O*-GlcNAc in many pathological processes (see Hart et al. 2007; Lefebvre et al. 2010 for review) including Alzheimer's disease (Griffith and Schmitz 1995; Yao and Coleman 1998; Liu et al. 2004; Yuzwa et al. 2008), cancer (Chou and Hart 2001; Donadio et al. 2008) and type II diabetes (McClain et al. 2002; Vosseller et al. 2002; Dias and Hart 2007; Macauley et al. 2008).

In contrast to phosphorylation, where over 500 kinases and 140 phosphatases are believed to act (Manning et al. 2002), in mammals just two enzymes are capable of modulating the *O*-GlcNAc modification. The enzyme responsible for the installation of the *O*-GlcNAc moiety is uridine diphospho-*N*-acetylglucosamine:polypeptide *β*-*N*-acetylglucosaminyltransferase (OGT) (Kreppel and Hart 1999; Lubas and Hanover 2000), whilst *O*-GlcNAcase (OGA) (Dong and Hart 1994) is responsible for its removal. In the CAZy classification of carbohydrate-active enzymes (http://www.cazy.org; Cantarel et al. 2009), OGA lies in family GH84, which also contains bacterial OGA homologues with high sequence identity to the domain of the human enzyme responsible for catalysis. This homology has facilitated structural analysis of enzyme–ligand complexes notably on the GH84 enzymes from *Bacteroides thetaiotaomicron* (*Bt*GH84) (Dennis et al. 2006) and *Clostridium perfringens* (NagJ) (Rao et al. 2006); recently reviewed in (Hurtado-Guerrero et al. 2008; Martinez-Fleites et al. 2010; Davies and Martinez-Fleites 2010). In the context of selective chemical intervention to modify cellular *O*-GlcNAc levels, OGA is a particularly attractive target, as Dong and Hart (1994) first noted, not least because glycoside hydrolases are more tractable targets for inhibition than glycosyltransferases. In addition, a chemical genetic approach to enzyme inhibition evades potential problems of alterations in protein–protein interactions that may occur in gene knockout or over-expression experiments (as is well documented in the kinase field, Knight and Shokat 2005). Enzyme inhibition, however, is not without drawbacks, as also illustrated by studies on phosphorylation (Knight and Shokat 2005). Inhibitors can be promiscuous and create complex phenotypes, a facet that is similarly beginning to emerge in the *O*-GlcNAc field (see, for example, Yamamoto et al. 1981; Kroncke et al. 1995; Macauley et al. 2008; Pathak et al. 2008; He et al. 2009; Macauley and Vocadlo 2010).

Inhibition of OGA with small molecules thus provides a way to increase cellular *O*-GlcNAc levels, which can aid understanding how the *O*-GlcNAc modification affects different processes in the cell; recent examples of this approach are described in Vosseller et al. (2002), Arias et al. (2004), Akimoto et al. (2007), Zou et al. (2007) and Yuzwa et al. (2008) and reviewed in Macauley and Vocadlo (2010). Generation of specific and potent inhibitors is thus of great interest to aid characterisation of the role *O*-GlcNAc plays in biological systems. An approach sometimes employed in the design of highly potent and selective inhibitors is to mimic the transition state (Pauling 1946), or closely related species, of the enzyme catalysed reaction (recently reviewed in a glycoside hydrolase context, Gloster and Davies 2010). Glycoside hydrolysis by OGA is accomplished with a double displacement "substrate-assisted catalysis", which was deduced using physical–organic methods (Macauley et al. 2005). Key features of this mechanism involve two neighbouring catalytic carboxylate-bearing residues in the enzyme active site, the substrate *N*-acetyl carbonyl acting as the catalytic nucleophile, and the formation of a bicyclic oxazoline intermediate. Our recent study (He et al. 2010), which examined the mechanistic details of *Bt*GH84 catalysis, revealed that the conformational itinerary (Fig. 1a) for this class of enzyme proceeds with a distorted $^{1,4}B/^{1}S_{3}$ conformation in the Michaelis complex, *via* a $^{4}C_{1}$ oxazoline intermediate, towards the formation of the *β*-linked product. This process involves two transition states with substantial oxocarbenium cation character. In the initial cyclisation step, the general acid Asp243 (*Bt*GH84 numbering) donates a proton to the *β*-linked glycosidic oxygen, whilst Asp242 assists the *N*-acetyl carbonyl for nucleophilic attack at the anomeric centre, resulting in cleavage of the glycosidic bond and formation of a high energy bicyclic oxazoline intermediate. In the subsequent ring-opening step, the deprotonated Asp243 now acts as a base assisting attack of a water molecule at the anomeric carbon, whilst the protonated Asp242 facilitates opening of the oxazoline ring to obtain the product with retained stereochemistry.

Glucono-1,5-lactone (**1a**) has been known for over half a century (Conchie and Levvy 1957; Lalegerie et al. 1982) as a glycosidase inhibitor. With an sp^2-hybridised carbon at the (pseudo) anomeric centre and the possibility for delocalisation/resonance (**1b**), glucono-1,5-lactone is thought to partially resemble the transition state oxocarbenium cation in terms of a distorted pyranose ring (Leaback 1968) and partial positive charge on the endocyclic oxygen (Reese et al. 1971). Glucono-1,5-lactone can, however, undergo hydrolysis in physiological conditions (Combes and Birch 1988), which hinders its usage for biological applications. Synthetic efforts have therefore been devoted to the development of analogues, such as the gluconolactams (**2** and **3**) (Inouye et al. 1968; Fleet et al. 1990; Overkleeft et al. 1993; Nishimura et al. 2000) and the lactone oximes (**4**–**7**) (Beer and Vasella 1985, 1986; Mohan and Vasella 2000; Stubbs et al. 2006). Of particular interest are the *N*-acetylglucosamine forms of these lactone oximes **5** and **7**, termed LOGNAc and PUGNAc, respectively (Beer et al. 1990). These are known inhibitors of *β*-*N*-acetylglucosaminidases (Horsch et al. 1991; Miller et al. 1993), including human OGA (Dong and Hart 1994; Gao et al. 2001; Macauley et al. 2005). The chemical structures for these inhibitors are shown in Fig. 1b.

Although kinetic data with *N*-acetyl lactone and lactam derivatives have been reported, dissection of the thermodynamics of inhibition and the conformation of these compounds in the active site of OGA or its homologues has rarely been investigated. Previously, the binding mode of PUGNAc with *Bt*GH84 has been presented (Macauley

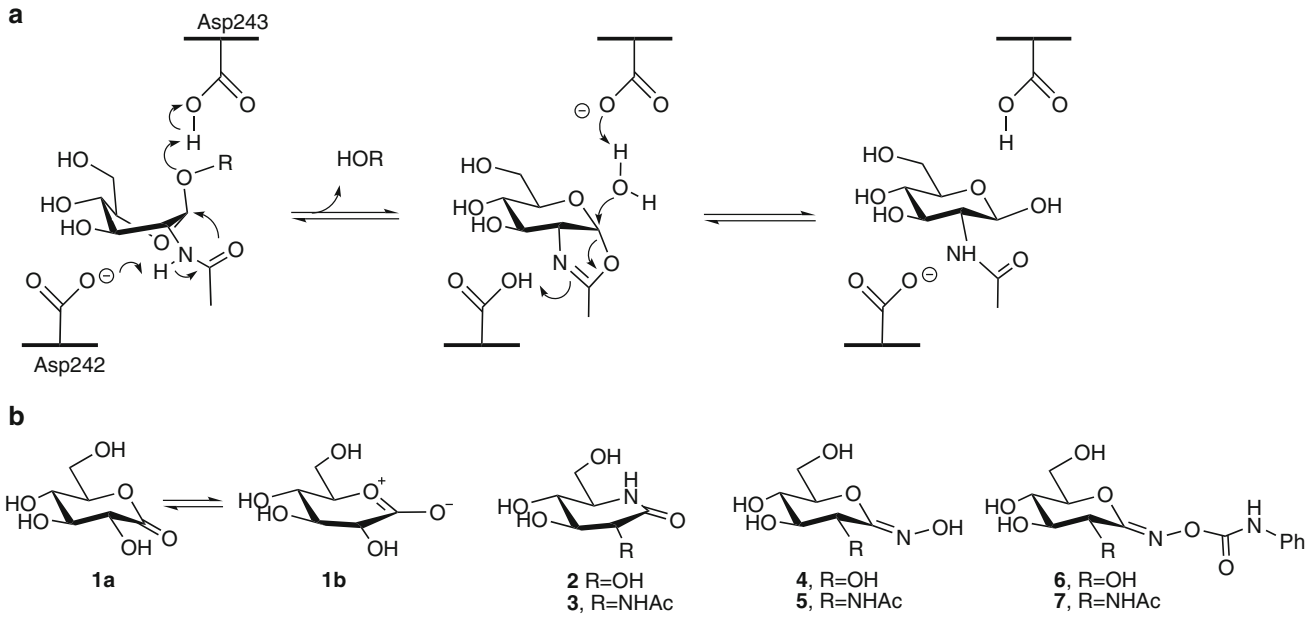

Fig. 1 The catalytic mechanism of OGA and inhibitors described in the text. **a** The two-step "substrate-assisted catalysis" utilised by OGA and its homologues in family GH84. In the first step, Asp243 (*Bt*GH84 numbering) acts as a general acid catalyst to aid departure of the leaving group. The adjacent Asp242 facilitates nucleophilic attack of the substrate 2-acetamido group to form an oxazoline intermediate. In the second step, Asp243 now acts as a general base, assisting the attack of an incoming water molecule at the anomeric centre to yield the product GlcNAc with retained β-configuration. Both steps involve a transition state with oxocarbenium ion character (not shown). **b** Inhibitors relevant to this study and described in the text are shown. (**1a**), glucono-1,5-lactone; (**1b**), resonance form of glucono-1,5-lactone; (**2**), glucono-1,5-lactam; (**3**), *N*-acetyl gluconolactam; (**4**), glucono-1,5-lactone oxime; (**5**), *N*-acetylglucosaminono-1,5-lactone (*Z*)-oxime (LOGNAc); (**6**), glucono-1,5-lactone phenylcarbamoyl oxime; (**7**), *N*-acetylglucosaminono-1,5-lactone *O*-(phenylcarbamoyl)-(*Z*)-oxime (PUGNAc)

et al. 2008). Here, we present the X-ray crystallographic structures of *N*-acetyl gluconolactam (**3**) and LOGNAc (**5**) in complex with *Bt*GH84. The inhibitory activities of these compounds, along with PUGNAc (**7**), are assessed by kinetics and the thermodynamic profiles are established with isothermal titration calorimetry (ITC). The results indicate that both **3** and **5** are poorer inhibitors of *Bt*GH84 than **7**, which is most likely due to their failure to capture key interactions with the catalytic acid, and the resultant steric clash with residues in the enzyme active site. The presence of a hydrophobic group in the +1 subsite (see Davies et al. 1997 for nomenclature), which facilitates substrate distortion and provides favourable interactions, as demonstrated by **7**, is therefore important. We hope these data will inform the process of rational inhibitor design for potential pharmaceutical applications.

Materials and methods

Inhibitors

N-acetyl gluconolactam (**3**), synthesised according to Granier and Vasella (1998), was a kind gift from Professor Andrea Vasella (ETH Zürich). LOGNAc (**5**) and PUGNAc (**7**) were synthesised using literature methods (Beer et al. 1990; Stubbs et al. 2006).

X-ray crystallography

N-terminal His_6-tagged recombinant *Bt*GH84 protein was expressed and purified as described previously (Dennis et al. 2006). To form inhibitor complexes, 10 mM of each compound was added to *Bt*GH84 prior to crystallisation. Crystals were grown using the hanging drop vapour diffusion method from a solution containing 15% PEG3350 (w/v), 0.1 M MES, pH 6.0, 0.3 M ammonium acetate and 10% glycerol. The same solution, but with the glycerol concentration raised to 20% (v/v), was used for cryo-protection before the crystals were flash frozen in liquid nitrogen. Diffraction data for *Bt*GH84 in complex with **3** and **5** were collected at the European Synchrotron Radiation Facility (ESRF, Grenoble) on beamlines ID14-2 and ID23-1, respectively. Data were integrated using MOSFLM and scaled with SCALA from the CCP4 suite (Collaborative Computational Project Number 4 1994) of programs. Structures were solved by molecular replacement methods using the *apo* *Bt*GH84

Table 1 Data collection and refinement statistics for *Bt*GH84 in complex with **3** and **5**

	*Bt*GH84 with **3**	*Bt*GH84 with **5**
Data collection		
Space group	P1	P1
Cell dimensions		
a, *b*, *c* (Å)	51.4, 94.1, 99.5	51.5, 93.5, 99.0
α, β, γ (°)	104.7, 94.0, 102.9	104.1, 94.3, 102.9
Resolution (Å)	49.63–2.00 (2.11–2.00)	44.65–1.95 (2.06–1.95)
R_{merge}	0.038 (0.15)	0.062 (0.31)
$I/\sigma I$	15.3 (4.9)	8.1 (2.3)
Completeness (%)	97.4 (96.5)	95.1 (93.8)
Redundancy	2.2 (2.2)	2.1 (2.1)
Refinement		
Resolution (Å)	2.0	1.95
No. reflections	108,848	113,702
R_{work}/R_{free}	0.18/0.22	0.18/0.22
RMS deviations		
Bond lengths (Å)	0.01	0.02
Bond angles (°)	1.3	1.3
PDB code	2XM1	2XM2

structure (PDB entry 2CHO) as the initial model. Manual corrections to the model were made with COOT (Emsley and Cowtan 2004). Cycles of restrained refinement were performed with REFMAC with TLS parameters (Winn et al. 2001) included in the later stages. Details of X-ray data and structure refinement statistics are given in Table 1.

Isothermal titration calorimetry

Isothermal titration calorimetry measurements were carried out in triplicate using a MicroCal VP calorimeter (Northampton, MA, USA). For sample preparation, purified *Bt*GH84 protein was extensively dialysed against 50 mM MES, pH 6.5 and 200 mM NaCl, and concentrated to 32–89 μM. Inhibitors were diluted into the same buffer to a final concentration of 0.5–1.0 mM. All samples were centrifuged and degassed prior to use. Titrations were performed by injection of 10 μL aliquots of the inhibitor into *Bt*GH84, at an interval of 4 min, with 307 rpm stirring speed. Experiments with **3** and **7** were carried out at 25°C, whilst measurements were also taken at 15 and 35°C for **5** (as no heat could be observed, see "Results"). The data were fitted to a non-linear regression model using Microcal Origin software, with stoichiometry (n), enthalpy (ΔH°) and association constant (K_a) as adjustable parameters. Other thermodynamic parameters were derived from the equation $-RT \ln K_a = \Delta G^\circ = \Delta H^\circ - T\Delta S^\circ$.

Kinetics

Kinetic studies of *Bt*GH84 were conducted by monitoring the change in UV–visible absorbance in thermally equilibrated disposable cuvettes using a Cintra 10 spectrophotometer. Assays were carried out at 25°C in a total volume of 1 mL buffer (50 mM MES, pH 6.5, 200 mM NaCl) with 50 μM 4-nitrophenyl *N*-acetyl D-glucosaminide (pNP-GlcNAc) as substrate. Reactions were initiated by the addition of 10 μL *Bt*GH84, using a syringe, to give a final concentration of 45 nM. Inhibitor concentrations in the assay varied from 10 to 100 μM for **5**, 0.5 to 7.5 μM for **3**, and 0.25 to 5 μM for **7** (in each case spanning the K_i value). 4-Nitrophenolate release was recorded continuously at 400 nm for 300 s. Rates were determined in both the presence and absence of inhibitor. The K_i value was determined using the following equation:

$$\frac{v_0}{v_i} = \frac{1}{K_i}[I] + 1$$

where v_0 and v_i are the rates of catalysis in the absence and presence of inhibitor, respectively. Under conditions where $[S] \ll K_M$, the fractional decrease in rate thus yields the K_i for a competitive inhibitor. A plot of v_0/v_i against inhibitor concentration yields a gradient of $1/K_i$, with an intercept of 1.

Results

Compounds *N*-acetyl gluconolactam (**3**), LOGNAc (**5**) and PUGNAc (**7**) were tested for their ability to inhibit *Bt*GH84 in a kinetic assay (Fig. 2), using pNP-GlcNAc as the substrate, which yielded K_i values of 920 nM for **7**, 2 μM for **3** and 24 μM for **5** (Table 2). ITC (Fig. 3) was performed (at the pH optimum for catalysis), which yielded K_d values for **7** and **3** (Table 2). The K_d values obtained using ITC are in reasonable agreement with the K_i values determined by kinetic means. ITC was also used to determine the thermodynamic parameters (enthalpy and derived entropy) of binding (Table 2). The thermodynamic signature for the binding of **3** with *Bt*GH84 is dominated by a large favourable enthalpy and a small favourable entropic contribution, whereas the binding of **7** is dominated by a favourable enthalpic contribution partially offset by unfavourable entropy. In our experiments, **5** yielded no heat change upon binding with *Bt*GH84 at 25°C, implying a ΔH° of 0. Experiments were repeated at both 15 and 35°C, where we hoped the significant heat capacity dependence on temperature would render ΔH° measurable, but still no heat change upon binding could be detected. If one assumes that the kinetic K_i is equivalent to the K_d determined by ITC, a ΔH° of 0 kcal/mol for LOGNAc binding

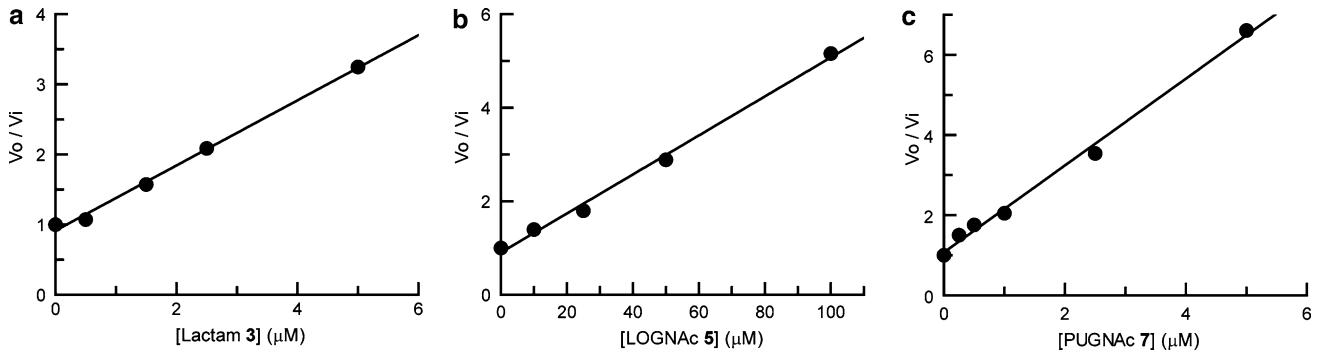

Fig. 2 Plot of v_0/v_i against inhibitor concentration for **a 3**, **b 5** and **c 7** with *Bt*GH84. Reaction rate is determined by measuring the release of 4-nitrophenolate in the absence (v_0) and presence (v_i) of inhibitor. The $1/K_i$ values for each compound were derived from the slope of the best fit line. Assays were carried out in 50 mM MES, pH 6.5, 200 mM NaCl

Table 2 Inhibition constants and thermodynamic data for compounds **3**, **5** and **7** binding to *Bt*GH84

Compound	*Bt*GH84				OGA K_i (μM)
	K_i (μM)	K_d (μM)	ΔH_a (kcal/mol)	$T\Delta S_a$ (kcal/mol)	
N-acetyl gluconolactam (**3**)	2	8.5 ± 3	−6.5 ± 0.4	+0.5	N/D
LOGNAc (**5**)	24	ND	(0)[c]	(+6.3)[c]	1.7[a]
PUGNAc (**7**)	0.92	2.5 ± 0.2	−10 ± 0.5	−2.3	0.050[a,b]

Values, where known, for the human *O*-GlcNAcase (OGA) are also shown

N/D Not determined

[a] Data from (Dong and Hart 1994)

[b] Data from (Macauley et al. 2005)

[c] No heat change was observed with **5** and *Bt*GH84. If a ΔH_a value of 0 is considered, and the K_d is assumed to be the same as the kinetically determined K_i, the $T\Delta S_a$ can be estimated

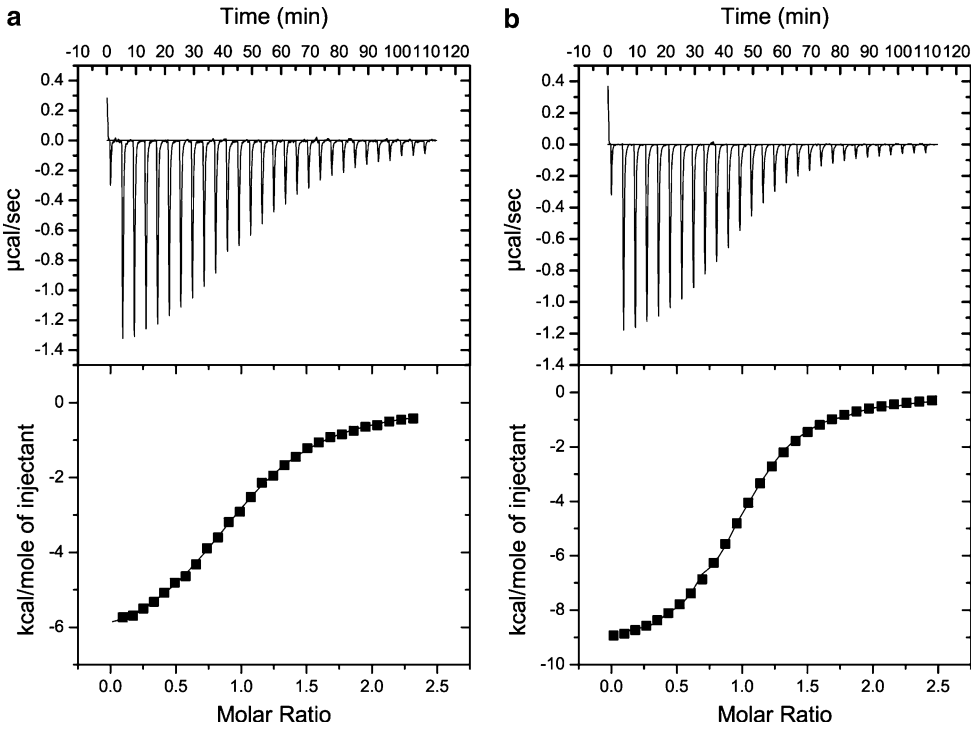

Fig. 3 Isothermal titration calorimetry plots for *Bt*GH84 with **a 3** and **b 7**. The *upper panel* shows the power supplied to the system to maintain a constant temperature against time (the area of each peak gives the heat of interaction for that injection). The *lower panel* shows the bimolecular fit of the normalised heats of interaction plotted against the molar concentration. Titrations were performed at 25°C in 50 mM MES, pH 6.5, 200 mM NaCl

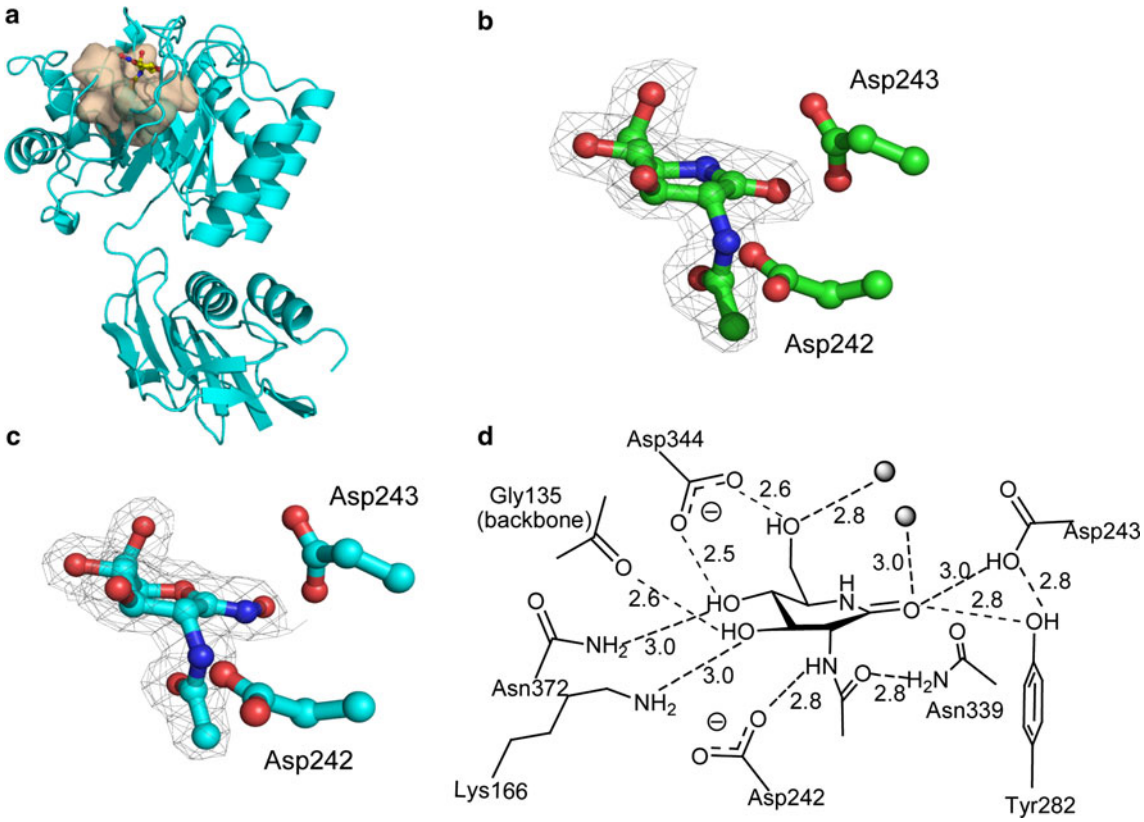

Fig. 4 **a** Cartoon representation of the *N*-terminal and catalytic domains of *Bt*GH84 (residues 4–372), in complex with LOGNAc (**5**), which highlights the active site pocket (shown in surface representation). Ball and stick representation of **b** **3** and **c** **5** bound to *Bt*GH84 (the key catalytic residues, Asp242 and Asp243, are shown). The observed electron density map ($2F_{obs} - F_{calc}$) is contoured at 1σ. Figures were made using PYMOL. **d** Schematic diagram of the interactions between **3** and *Bt*GH84

to *Bt*GH84 implies a favourable $T\Delta S$ of approximately +6.3 kcal/mol.

The X-ray crystal structures of *Bt*GH84 (Fig. 4) in complex with LOGNAc (**5**) and *N*-acetyl gluconolactam (**3**) were determined to 1.95 and 2 Å resolution, respectively (Table 1; the PUGNAc complex has been reported previously; Macauley et al. 2008). *N*-acetyl gluconolactam (**3**) (Fig. 4b) is found in a ^4E (envelope) conformation, which is consistent with the $^4H_3$ half-chair structure of the parent gluconolactam (Inouye et al. 1968). The O6 hydroxyl group of **3** receives a hydrogen bond from a water molecule, sitting above the plane, and donates a hydrogen bond to Asp344 (Fig. 4d). The O4 hydroxyl group is engaged in two hydrogen bonds with Asn344 and Asn372, and the O3 hydroxyl group interacts with the main chain carbonyl of Gly135 and the side chain of Lys166. The 2-acetamido group of **3**, sandwiched by Trp337 and Tyr282 in a hydrophobic pocket, accepts a hydrogen bond from Asn339 on its carbonyl oxygen, whilst the hydrogen atom on the nitrogen in the 2-acetamido group provides a hydrogen bond to residue Asp242. Intriguing features in the complex with **3** are an "over-coordinated" exocyclic carbonyl (involved in 3 hydrogen bonds: with an incoming water, the catalytic acid/base Asp243 and Tyr282) and bifurcated hydrogen bonds formed between the Asp243 carboxyl group, the exocyclic carbonyl oxygen and the Tyr282 hydroxyl group. As a crystal structure reflects an average arrangement of all molecules in the crystal lattice, the interactions observed here may imply a dynamic motion of the hydrogen bond network between Tyr282, Asp243 and a water molecule in the active site. This is supported by the observation that the catalytic acid/base Asp243 has a higher B factor (34 Å^2 in molecule A and 25 Å^2 in molecule B, and two conformations can be seen in the latter) than the surrounding residues, and the water molecule is also partially occupied. These movements in *Bt*GH84 caused by potential clashes with the carbonyl group of **3** are likely to contribute to the reduced potency compared to **7**. Indeed, the presence of an equatorial group at the anomeric position is possibly a drawback of many compounds, as it places the hydrogen bonding acceptor in the plane of the pyranoside; in the Michaelis complex or transition state, however, the departing oxygen is pseudo-axial "above" the ring (see He et al. 2010; Vocadlo and Davies 2008 for review).

Similarly to the *N*-acetyl gluconolactam (**3**), electron density clearly revealed the presence of LOGNAc (**5**)

bound in the active site of *Bt*GH84, in a ^4E conformation (Fig. 4c), which reflects some distortion of the lactone oxime away from the favoured $^4C_1$ chair conformation (see "Discussion" below). LOGNAc (**5**) hydrogen bonds with a number of active site residues of *Bt*GH84 and two water molecules (the interactions are the same as described for **3**, except for those with the lactam group). The oxime nitrogen, which mimics the glycosidic oxygen in the substrate, is within hydrogen bonding distance to Tyr282, and potentially with Asp243 and a water molecule above the plane (although both Asp243 and the water molecule show high mobility and the distances to the oxime nitrogen vary between the 2 molecules in the asymmetric unit). The hydroxyl group attached to the oxime nitrogen coordinates with Tyr282 and a water molecule, most likely in a *Z*-configuration, although the density for this atom is substantially (and surprisingly) weaker than for the rest of the inhibitor, which may reflect X-ray induced decay of the compound (the complex was repeated 3 times with different independent samples of material and the same weak density was observed in all cases).

Discussion

A common feature of both lactone oximes and lactams, in terms of chemical structure, is the presence of an exocyclic heteroatom (O or N) next to the "anomeric" carbon centre, which mimics the glycosidic oxygen atom. Due to the sp^2 hybridisation with this heteroatom, and the absence of a 1-H substituent, it is likely that both **3** and **5** have a lower energy barrier to ring distortion than a pyranoside, which is reflected in the ^4E conformations observed "on-enzyme" for both compounds. Solution or small molecule structures, of lactams such as **3** have been shown to favour a $^4H_3$ conformation (Inouye et al. 1968; Nishimura et al. 2000). Although **5** may be easily distorted in solution, as evidenced in an NMR study (Beer and Vasella 1986), it has preference towards a $^4C_1$ chair, as demonstrated by the solid state structure of a closely related compound (Hoos et al. 1993) and in the protein complex of **5** with glycogen phosphorylase (Papageorgiou et al. 1991). As **5** favours a chair in solid state, but one that may be distorted, it could be that delocalisation of the amide of **3** is more facile, thus favouring a half-chair conformation, and this may contribute in part to the better binding of **3** in these experiments.

Given the poor inhibition by LOGNAc (**5**), it is surprising that PUGNAc (**7**) is such a strong OGA inhibitor (although inhibition of *Bt*GH84 is weaker than human OGA). No doubt, this reflects the addition of the aglycone-mimicking *N*-phenylcarbamate moiety on **7** that extends out of the active site pocket and, in addition to aromatic interactions, makes several hydrogen bond interactions with residues including His433, Tyr282 and Asp243. Similar to the hydrogen bond observed between Asp243 and the glycosidic oxygen in the Michaelis complex with *Bt*GH84 (He et al. 2010) (Fig. 5a), Asp243 in the structure of the PUGNAc complex donates a proton to the lone pair of electrons on the sp^2 hybridised nitrogen through its Oδ2 atom. However, the equivalent interaction in the complexes with **3** and **5** are with the Oδ1 atom of Asp243, and neither

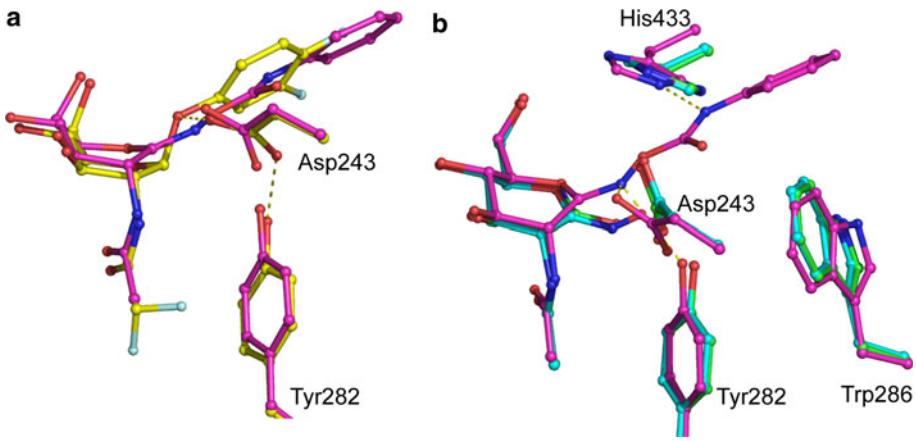

Fig. 5 **a** Structure of *Bt*GH84 in complex with PUGNAc (*purple*) superimposed with the Michaelis complex (*yellow*). The aglycone moiety of PUGNAc resembles the leaving group in the Michaelis complex in terms of conformation ($^{1,4}B$) and the pseudo-axial position of the group in the +1 subsite, which allows a hydrogen bond interaction (represented by a *dashed line*) between the catalytic acid (Asp243) and the glycosidic oxygen atom in the Michaelis complex. **b** Superimposition of *Bt*GH84 in complex with PUGNAc (**7**) (*purple*), LOGNAc (**5**) (*cyan*), and *N*-acetyl gluconolactam (**3**) (*green*). **3** and **5** are bound in a ^4E conformation, causing the pseudo-glycosidic oxygen atom to lie in the plane of the glycoside, which is sterically unfavoured by the enzyme. **7** is distorted towards a $^{1,4}B$ conformation, and its *N*-phenylcarbamate group makes hydrophobic interactions with Trp286 and favourable hydrogen bond interactions (shown by *dashed lines*) with active site residues (His433, Asp243, and Tyr282)

satisfies optimum hydrogen bond geometry. The binding of the *N*-phenylcarbamate group of **7** in the aglycone subsites appears to be sufficient to distort the pyranose ring of **7** away from its favoured $^4C_1$ chair, and beyond the ^4E conformation observed in the complex with **5**, towards a $^{1,4}B$ conformation (Fig. 5b). This distortion means that the aglycone is almost pseudo-axial and allows the hydrogen bond between the exocyclic heteroatom nitrogen atom (corresponding to the glycosidic oxygen in the substrate) and catalytic acid Asp243. Such distortion also avoids any steric clash with enzyme active site residues (as **7** is elevated in the active site pocket; Trp286 and Asp243 are also slightly perturbed from their position compared to what is observed with other inhibitors). It is becoming apparent, from diverse complexes with both *Bt*GH84 (imidazole-PUGNAc hybrid, Shanmugasundaram et al. 2006; *N*-butyryl-PUGNAc, Balcewich et al. 2009) and *C. perfringens* NagJ (PUGNAc, Rao et al. 2006; GlcNAcstatins, Dorfmueller et al. 2006, 2009) that pseudo-aglycone moieties provide additional binding energy to facilitate distortion, causing reorientation of the sugar ring and thus allowing the pseudo-glycosidic atom to interact with the catalytic acid. This important interaction (see Heightman and Vasella 1999; Vasella et al. 2002 for reviews) is not captured to the same extent in the complex with compounds **3** and **5**. In contrast, the sp^3 pseudo-anomeric centre of a 1-acetamido derivative of 6-epivalienamine (Scaffidi et al. 2007) is more capable of forming this interaction, as can some azepane derivatives (Marcelo et al. 2009), but is at the expense of the distorted half-chair or envelope geometry. PUGNAc (**7**) is a weaker inhibitor of *Bt*GH84 than human OGA, which may reflect a difference in the interactions formed in the +1 (aglycone) subsites. Although the critical −1 subsite of *Bt*GH84 is invariant with the human enzyme (based on sequence alignments), in the +1 subsite Trp286 of *Bt*GH84 is equivalent to a Phe in human OGA. In addition, **7** was observed to bind differently in the aglycone subsite of *Bt*GH84 (Macauley et al. 2008) and NagJ (Rao et al. 2006). The diverse binding constants are therefore not surprising given the adventitious nature of the pseudo-aglycone interactions.

LOGNAc (**5**) binds ten-fold less tightly to *Bt*GH84 than *N*-acetyl gluconolactam (**3**). This result agrees with an earlier report in which **5** was shown to inhibit diverse *β*-*N*-acetylglucosaminidases of animal, higher plant and fungus origin only 40–70% as effectively as an *N*-acetyl-glucosaminono-1,5-lactone (Horsch et al. 1991). A similar situation pertains for the *gluco*-variant where the inhibition of sweet-almond *β*-glucosidase by 1,5-lactone oxime (**4**) is ten-fold weaker than the parent glucono-1,5-lactone (**2**) (Heightman and Vasella 1999). This suggests that the additional hydroxyl group may not promote favourable interactions in the active site of enzymes. Indeed, when LOGNAc is bound in a ^4E conformation in the complex with *Bt*GH84, the hydroximonyl group is closely surrounded by Val314, Asp243 and Tyr282 where interactions are not sterically optimal.

The thermodynamic signature for **3** and **7** with *Bt*GH84 revealed that the binding for both is dominated by enthalpy. Large enthalpic contributions to binding have been demonstrated extensively for a number of inhibitors with glycoside hydrolases previously (Gloster et al. 2007). However, it is interesting that other inhibitors studied which bear a hydrophobic group protruding into the +1 subsite have significant entropic contributions to binding, but the same is not true for **7** with *Bt*GH84 in this case. Large beneficial entropic contributions, on other systems, have been interpreted as reflecting the beneficial desolvation of inhibitor or protein residues upon inhibitor binding, where that inhibitor itself remains flexible (Gloster et al. 2007). It is therefore possible that binding of the *N*-phenylcarbamoyl group of **7** in the active site of *Bt*GH84 is associated with a considerable reduction in mobility compared to some of the aryl-group bearing inhibitors described in Gloster et al. (2007). That the *N*-butyl PUGNAc complex of *Bt*GH84 binds, however, with the *N*-phenylcarbamoyl group in a completely different orientation certainly hints at an inherent flexibility of this group (PDB code: 2wca). The fact that no heat changes could be observed with **5** binding to *Bt*GH84 suggests that it has no enthalpic contribution to binding and is driven by entropy under the conditions used. This is unusual for glycosidase inhibitors and to our knowledge has only been observed previously with a castanospermine analogue bearing an octyl chain; here, tight binding was attributed to desolvation of the protein residues upon binding the large aliphatic group (Aguilar-Moncayo et al. 2009). For compound **5**, however, the reasoning is more difficult to fathom. As demonstrated in the structure of the complex, a number of hydrogen bond interactions are formed between **5** and active site residues, which, one would assume, would be reflected in a measurable enthalpy by ITC. **5** does bind to two water molecules, but this is the same as for **3**, which has a significant enthalpic contribution to binding. The reasons for its net ΔH of zero remain unclear.

The analysis of the binding of *N*-acetyl gluconolactam (**3**) and LOGNAc (**5**) to *Bt*GH84 presented here shows that, consistent with past reports, neither are tight-binding inhibitors. The work shows that these inhibitors, with sp^2 pseudo-anomeric centres, are unable to capture the binding energy of the mechanistically designed inhibitors such as GlcNAc-thiazoline, its analogues (Macauley et al. 2005; Dennis et al. 2006), and the isothiourea containing Thiamet-G (Yuzwa et al. 2008). Thus, to generate sufficient binding energy, the lactone oxime needs to be further

functionalised to generate PUGNAc, in which adventitious interactions in the +1 subsite benefit binding 30-fold. Similar situations in which a poor(er) inhibitor is enhanced through the capture of +1 subsite interactions has been observed on other glycosidase systems including β-glucosidases (Hrmova et al. 2004; Hrmova et al. 2005; Gloster et al. 2007) and β-mannosidases (Tailford et al. 2008). Comparison of the Michaelis and PUGNAc complexes of *Bt*GH84 reveals different positions for the phenyl rings with that of PUGNAc displaced 3.4 Å from the phenyl ring of the former and extended further out of the +1 subsite (Fig. 5a). Such a positional difference, coupled to opportunities for bicyclic ring systems and linkers optimised for their adventitious interactions, offer considerable prospects for both structure-inspired and combinatorial approaches to generate more potent inhibitors of human OGA in the future.

Acknowledgments The authors thank the Biotechnology and Biological Sciences Research Council for their funding. G. J. D. is a Royal Society Wolfson Research Merit Award recipient. Y. H. was partially supported by the Wild Fund of the Department of Chemistry at York. T. M. G. is a Sir Henry Wellcome Postdoctoral Fellow, funded by the Wellcome Trust. Professor Andrea Vasella (ETH Zürich) is thanked for provision of *N*-acetyl gluconolactam **3**.

References

Aguilar-Moncayo M, Gloster TM, Turkenburg JP, García-Moreno MI, Ortiz Mellet C, Davies GJ, Fernádez G (2009) Glycosidase inhibition by ring-modified castanospermine analogues: tackling enzyme selectivity by inhibitor tailoring. Org Biomol Chem 7:2738–2747

Akimoto Y, Hart GW, Wells L, Vosseller K, Yamamoto K, Munetomo E, Ohara-Imaizumi M, Nishiwaki C, Nagamatsu S, Hirano H et al (2007) Elevation of the post-translational modification of proteins by *O*-linked *N*-acetylglucosamine leads to deterioration of the glucose-stimulated insulin secretion in the pancreas of diabetic Goto-Kakizaki rats. Glycobiology 17:127–140

Arias EB, Kim J, Cartee GD (2004) Prolonged incubation in PUGNAc results in increased protein *O*-linked glycosylation and insulin resistance in rat skeletal muscle. Diabetes 53:921–930

Balcewich MD, Stubbs KA, He Y, James TW, Davies GJ, Vocadlo DJ, Mark BL (2009) Insight into a strategy for attenuating AmpC-mediated β-lactam resistance: structural basis for selective inhibition of the glycoside hydrolase NagZ. Prot Sci 18:1541–1551

Beer D, Vasella A (1985) Aldonhydroximo-lactones—preparation and determination of configuration. Helv Chim Acta 68:2254–2274

Beer D, Vasella A (1986) Inhibition of emulsion by D-gluconhydroximo-1,5-lactone and related compounds. Helv Chim Acta 69:267–270

Beer D, Maloisel JL, Rast DM, Vasella A (1990) Synthesis of 2-acetamido-2-deoxy-D-gluconhydroximolactone-derived and chitobionhydroximolactone-derived *N*-phenylcarbamates, potential inhibitors of beta-*N*-acetylglucosaminidase. Helv Chim Acta 73:1918–1922

Butkinaree C, Park K, Hart GW (2010) *O*-linked beta-*N*-acetylglucosamine (*O*-GlcNAc): extensive crosstalk with phosphorylation to regulate signaling and transcription in response to nutrients and stress. Biochim Biophys Acta 1800:96–106

Cantarel BL, Coutinho PM, Rancurel C, Bernard T, Lombard V, Henrissat B (2009) The Carbohydrate-Active EnZymes database (CAZy): an expert resource for glycogenomics. Nucleic Acids Res 37:D233–D238

Chou TY, Hart GW (2001) *O*-linked *N*-acetylglucosamine and cancer: messages from the glycosylation of c-Myc. Adv Exp Med Biol 491:413–418

Collaborative Computational Project Number 4 (1994) The CCP4 suite: programs for protein crystallography. Acta Crystallogr D50:760–763

Combes CL, Birch GG (1988) Interaction of D-glucono-1,5-lactone with water. Food Chem 27:283–298

Conchie J, Levvy GA (1957) Inhibition of glycosidases by aldonolactones of corresponding configuration. Biochem J 65:389–395

Davies GJ, Martinez-Fleites C (2010) The *O*-GlcNAc modification: 3-D structure, enzymology and the development of selective inhibitors to probe disease. Biochem Soc Trans (in press)

Davies GJ, Wilson KS, Henrissat B (1997) Nomenclature for sugar-binding subsites in glycosyl hydrolases. Biochem J 321:557–559

Dennis RJ, Taylor EJ, Macauley MS, Stubbs KA, Turkenburg JP, Hart SJ, Black GN, Vocadlo DJ, Davies GJ (2006) Structure and mechanism of a bacterial beta-glucosaminidase having *O*-GlcNAcase activity. Nat Struct Mol Biol 13:365–371

Dias WB, Hart GW (2007) *O*-GlcNAc modification in diabetes and Alzheimer's disease. Mol Biosyst 3:766–772

Donadio AC, Lobo C, Tosina M, de la Rosa V, Martin-Rufian M, Campos-Sandoval JA, Mates JM, Marquez J, Alonso FJ, Segura JA (2008) Antisense glutaminase inhibition modifies the *O*-GlcNAc pattern and flux through the hexosamine pathway in breast cancer cells. J Cell Biochem 103:800–811

Dong DL, Hart GW (1994) Purification and characterization of an *O*-GlcNAc selective *N*-acetyl-beta-D-glucosaminidase from rat spleen cytosol. J Biol Chem 269:19321–19330

Dorfmueller HC, Borodkin VS, Schimpl M, Shepherd SM, Shpiro NA, van Aalten DM (2006) GlcNAcstatin: a picomolar, selective *O*-GlcNAcase inhibitor that modulates intracellular *O*-glcNAcylation levels. J Am Chem Soc 128:16484–16485

Dorfmueller HC, Borodkin VS, Schimpl M, van Aalten DM (2009) GlcNAcstatins are nanomolar inhibitors of human *O*-GlcNAcase inducing cellular hyper-*O*-GlcNAcylation. Biochem J 420:221–227

Emsley P, Cowtan K (2004) Coot: model-building tools for molecular graphics. Acta Crystallogr D60:2126–2132

Fleet GWJ, Carpenter NM, Petursson S, Ramsden NG (1990) Synthesis of deoxynojirimycin and of nojirimycin delta-lactam. Tetrahedron Lett 31:409–412

Gao Y, Wells L, Comer FI, Parker GJ, Hart GW (2001) Dynamic *O*-glycosylation of nuclear and cytosolic proteins: cloning and characterization of a neutral, cytosolic beta-*N*-acetylglucosaminidase from human brain. J Biol Chem 276:9838–9845

Gloster TM, Davies GJ (2010) Glycosidase inhibition: assessing mimicry of the transition state. Org Biomol Chem 8:305–320

Gloster TM, Meloncelli P, Stick R, Zechel D, Vasella A, Davies GJ (2007) Glycosidase inhibition: an assessment of the binding of eighteen putative transition-state mimics. J Am Chem Soc 129:2345–2354

Granier T, Vasella A (1998) Synthesis and some transformations of 2-acetamido-5-amino-3,4,6-tri-*O*-benzyl-2,5-dideoxy-D-gluconο-1, 5-lactam. Helv Chim Acta 81:865–880

Griffith LS, Schmitz B (1995) *O*-linked *N*-acetylglucosamine is upregulated in Alzheimer brains. Biochem Biophys Res Commun 213:424–431

Hart GW, Housley MP, Slawson C (2007) Cycling of *O*-linked beta-*N*-acetylglucosamine on nucleocytoplasmic proteins. Nature 446:1017–1022

He Y, Martinez-Fleites C, Bubb A, Gloster TM, Davies GJ (2009) Structural insight into the mechanism of streptozotocin inhibition of *O*-GlcNAcase. Carbohydr Res 344:627–631

He Y, Macauley MS, Stubbs KA, Vocadlo DJ, Davies GJ (2010) Visualizing the reaction coordinate of an *O*-GlcNAc hydrolase. J Am Chem Soc 132:1807–1809

Heightman TD, Vasella AT (1999) Recent insights into inhibition, structure, and mechanism of configuration-retaining glycosidases. Angew Chem Int Ed 38:750–770

Hoos R, Naughton AB, Thiel W, Vasella A, Weber W, Rupitz K, Withers SG (1993) D-Gluconhydroximo-1, 5-lactam and related *N*-arylcarbamates—theoretical calculations, structure, synthesis, and inhibitory effect on beta-glucosidases. Helv Chim Acta 76:2666–2686

Horsch M, Hoesch L, Vasella A, Rast DM (1991) *N*-acetylglucosaminono-1,5-lactone oxime and the corresponding (phenylcarbamoyl)oxime novel and potent inhibitors of beta-*N*-acetylglucosaminidase. Eur J Biochem 197:815–818

Hrmova M, de Gori R, Smith BJ, Vasella A, Vargese JN, Fincher GB (2004) Three-dimensional structure of the barley β-D-glucan glucohydrolase in complex with a transition state mimic. J Biol Chem 279:4970–4980

Hrmova M, Streltsov VA, Smith BJ, Vasella A, Vargese JN, Fincher GB (2005) Structural rationale for low-nanomolar binding of transition state mimics to a family GH3 β-D-glucan glucohydrolase from barley. Biochemistry 44:16529–16539

Hurtado-Guerrero R, Dorfmueller HC, van Aalten DM (2008) Molecular mechanisms of *O*-GlcNAcylation. Curr Opin Struct Biol 18:551–557

Inouye S, Tsuruoka T, Ito T, Niida T (1968) Structure and synthesis of nojirimycin. Tetrahedron 24:2125

Knight ZA, Shokat KM (2005) Features of selective kinase inhibitors. Chem Biol 12:621–637

Kreppel LK, Hart GW (1999) Regulation of a cytosolic and nuclear *O*-GlcNAc transferase. Role of the tetratricopeptide repeats. J Biol Chem 274:32015–32022

Kroncke KD, Fehsel K, Sommer A, Rodriguez ML, Kolb-Bachofen V (1995) Nitric oxide generation during cellular metabolization of the diabetogenic *N*-methyl-*N*-nitroso-urea streptozotozin contributes to islet cell DNA damage. Biol Chem Hoppe Seyler 376:179–185

Lalegerie P, Legler G, Yon JM (1982) The use of inhibitors in the study of glycosidases. Biochimie 64:977–1000

Leaback DH (1968) On the inhibition of beta-*N*-acetyl-D-glucosaminidase by 2-acetamido-2-deoxy-D-glucono-(1,5)-lactone. Biochem Biophys Res Commun 32:1025–1030

Lefebvre T, Dehennaut V, Guinez C, Olivier S, Drougat L, Mir A-M, Mortuaire M, Vercoutter-Edouart A-S, Michalski J-C (2010) Dysregulation of the nutrient/stress sensor *O*-GlcNAcylation is involved in the etiology of cardiovascular disorders, type-2 diabetes and Alzheimer's disease. Biochim Biophys Acta 1800:67–79

Liu F, Iqbal K, Grundke-Iqbal I, Hart GW, Gong CX (2004) *O*-GlcNAcylation regulates phosphorylation of tau: a mechanism involved in Alzheimer's disease. Proc Natl Acad Sci USA 101:10804–10809

Lubas WA, Hanover JA (2000) Functional expression of *O*-linked GlcNAc transferase. Domain structure and substrate specificity. J Biol Chem 275:10983–10988

Macauley MS, Vocadlo DJ (2010) Increasing *O*-GlcNAc levels: an overview of small-molecule inhibitors of *O*-GlcNAcase. Biochim Biophys Acta 1800:107–121

Macauley MS, Whitworth GE, Debowski AW, Chin D, Vocadlo DJ (2005) *O*-GlcNAcase uses substrate-assisted catalysis: kinetic analysis and development of highly selective mechanism-inspired inhibitors. J Biol Chem 280:25313–25322

Macauley MS, Bubb AK, Martinez-Fleites C, Davies GJ, Vocadlo DJ (2008) Elevation of global *O*-GlcNAc levels in 3T3-L1 adipocytes by selective inhibition of *O*-GlcNAcase does not induce insulin resistance. J Biol Chem 283:34687–34695

Manning G, Whyte DB, Martinez R, Hunter T, Sudarsanam S (2002) The protein kinase complement of the human genome. Science 298:1912–1934

Marcelo F, He Y, Yuzwa SA, Nieto L, Jiménez-Barbero J, Sollogoub M, Vocadlo DJ, Davies GJ, Blériot Y (2009) Molecular basis for inhibition of GH84 glycoside hydrolases by substituted azepanes: conformational flexibility enables probing of substrate distortion. J Am Chem Soc 131:5390–5392

Martinez-Fleites C, He Y, Davies GJ (2010) Structural analyses of enzymes involved in the *O*-GlcNAc modification. Biochim Biophys Acta 1800:122–133

McClain DA, Lubas WA, Cooksey RC, Hazel M, Parker GJ, Love DC, Hanover JA (2002) Altered glycan-dependent signaling induces insulin resistance and hyperleptinemia. Proc Natl Acad Sci USA 99:10695–10699

Miller DJ, Gong X, Shur BD (1993) Sperm require beta-*N*-acetylglucosaminidase to penetrate through the egg zona pellucida. Development 118:1279–1289

Mohan H, Vasella A (2000) An improved synthesis of 2-acetamido-2-deoxy-D-gluconohydroximolactone (PUGNAc), a strong inhibitor of beta-*N*-acetylglucosaminidases. Helv Chim Acta 83:114–118

Nishimura Y, Adachi H, Satoh T, Shitara E, Nakamura H, Kojima F, Takeuchi T (2000) All eight stereoisomeric D-glyconic-delta-lactams: synthesis, conformational analysis, and evaluation as glycosidase inhibitors. J Org Chem 65:4871–4882

Olszewski NE, West CM, Sassi SO, Hartweck LM (2010) *O*-GlcNAc protein modification in plants: evolution and function. Biochim Biophys Acta 1800:49–56

Overkleeft HS, Vanwiltenburg J, Pandit UK (1993) An expedient stereoselective synthesis of gluconolactam. Tetrahedron Lett 34:2527–2528

Papageorgiou AC, Oikonomakos NG, Leonidas DD, Bernet B, Beer D, Vasella A (1991) The binding of D-gluconohydroximo-1,5-lactone to glycogen-phosphorylase—kinetic, ultracentrifugation and crystallographic studies. Biochem J 274:329–338

Pathak S, Dorfmueller HC, Borodkin VS, van Aalten DM (2008) Chemical dissection of the link between streptozotocin, *O*-GlcNAc, and pancreatic cell death. Chem Biol 15:799–807

Pauling L (1946) Molecular architecture and biological reactions. Chem Eng News 24:1375–1377

Rao FV, Dorfmueller HC, Villa F, Allwood M, Eggleston IM, van Aalten DM (2006) Structural insights into the mechanism and inhibition of eukaryotic *O*-GlcNAc hydrolysis. EMBO J 25:1569–1578

Reese ET, Parrish FW, Ettlinger M (1971) Nojirimycin and D-glucono-1,5-lactone as inhibitors of carbohydrases. Carbohydr Res 18:381–388

Scaffidi A, Stubbs KA, Dennis RJ, Taylor EJ, Davies GJ, Vocadlo DJ, Stick RV (2007) A 1-acetamido derivative of 6-epivalienamine: an inhibitor of a diverse array of β-*N*-acetylglucosaminidases. Org Biomol Chem 5:3013–3019

Shanmugasundaram B, Debowski AW, Dennis RJ, Davies GJ, Vocadlo DJ, Vasella A (2006) Inhibition of *O*-GlcNAcase by a *gluco*-configured nagstatin and a PUGNAc–imidazole hybrid inhibitor. Chem Commun 4372–4374

Stubbs KA, Zhang N, Vocadlo DJ (2006) A divergent synthesis of 2-acyl derivatives of PUGNAc yields selective inhibitors of *O*-GlcNAcase. Org Biomol Chem 4:839–845

Tailford LN, Offen WA, Smith NL, Dumon C, Morland C, Gratien J, Heck M-P, Stick RV, Blériot Y, Vasella A et al (2008) Structural

and biochemical evidence for a boat-like transition state in β-mannosidases. Nat Chem Biol 4:306–312

Torres CR, Hart GW (1984) Topography and polypeptide distribution of terminal *N*-acetylglucosamine residues on the surfaces of intact lymphocytes. Evidence for *O*-linked GlcNAc. J Biol Chem 259:3308–3317

Vasella A, Davies G, Böhm M (2002) Glycosidase mechanisms. Curr Opin Chem Biol 6:619–629

Vocadlo D, Davies GJ (2008) Mechanistic insights into glycosidase chemistry. Curr Opin Chem Biol 12:539–555

Vosseller K, Wells L, Lane MD, Hart GW (2002) Elevated nucleocytoplasmic glycosylation by *O*-GlcNAc results in insulin resistance associated with defects in Akt activation in 3T3-L1 adipocytes. Proc Natl Acad Sci USA 99:5313–5318

Wells L, Vosseller K, Hart GW (2001) Glycosylation of nucleocytoplasmic proteins: signal transduction and *O*-GlcNAc. Science 291:2376–2378

Winn MD, Isupov MN, Murshudov GN (2001) Use of TLS parameters to model anisotropic displacements in macromolecular refinement. Acta Crystallogr D 57:122–133

Yamamoto H, Uchigata Y, Okamoto H (1981) Streptozotocin and alloxan induce DNA strand breaks and poly(ADP-ribose) synthetase in pancreatic islets. Nature 294:284–286

Yao PJ, Coleman PD (1998) Reduction of *O*-linked *N*-acetylglucosamine-modified assembly protein-3 in Alzheimer's disease. J Neurosci 18:2399–2411

Yuzwa SA, Macauley MS, Heinonen JE, Shan X, Dennis RJ, He Y, Whitworth GE, Stubbs KA, McEachern EJ, Davies GJ et al (2008) A potent mechanism-inspired *O*-GlcNAcase inhibitor that blocks phosphorylation of tau in vivo. Nat Chem Biol 4:483–490

Zou L, Yang S, Hu S, Chaudry IH, Marchase RB, Chatham JC (2007) The protective effects of PUGNAc on cardiac function after trauma-hemorrhage are mediated via increased protein *O*-GlcNAc levels. Shock 27:402–408